Intron-containing RNA from the HIV-1 provirus activates type I interferon and inflammatory cytokines

Sean Matthew McCauley[1], Kyusik Kim[1], Anetta Nowosielska[1], Ann Dauphin[1], William Edward Diehl[1], and Jeremy Luban[1,2]*

Author Affiliations:

[1]Program in Molecular Medicine, University of Massachusetts Medical School, Worcester, MA 01605, USA

[2]Department of Biochemistry and Molecular Pharmacology, University of Massachusetts Medical School, Worcester, MA 01605, USA

*Corresponding author email: jeremy.luban@umassmed.edu

ABSTRACT

HIV-1-infected people who take antiviral drugs that render viremia undetectable have ongoing inflammation of unknown etiology. The HIV-1 provirus, a permanent genetic element in long-lived cells of the immune system, is not eliminated by antiviral drugs, and is therefore a possible contributor to this inflammation. Most HIV-1 proviruses in infected people are replication defective but many are transcriptionally active. We found that the HIV-1 provirus activated innate immune signaling in dendritic cells, macrophages, and $CD4^+$ T cells. Immune activation required HIV-1 provirus transcription and expression of CRM1-dependent, Rev-dependent, RRE-containing, unspliced HIV-1 RNA. If *rev* was provided in *trans*, all HIV-1 coding sequences were dispensable except those *cis*-acting sequences required for replication or splicing. These results indicate that Rev-dependent, intron-containing, HIV-1 RNA is detected by the innate immune system, and that drugs which inhibit HIV-1 transcription or Rev-dependent, HIV-1 RNA metabolism, would add qualitative benefit to current antiviral drug regimens.

INTRODUCTION

Drugs that block activity of the three HIV-1 enzymes - reverse transcriptase, integrase, and protease - potently suppress HIV-1 viremia and protect infected people from developing AIDS (Günthard et al., 2016). Despite effective antiviral therapy, many patients have systemic inflammation associated with increased risk of cardiovascular pathology (Freiberg et al., 2013). Plausible explanations for this inflammation include ongoing T cell dysfunction, disruption of intestinal epithelium integrity, lymphatic tissue fibrosis, antiviral drug toxicity, and co-morbid infections such as cytomegalovirus (Brenchley et al., 2006; Hunt et al., 2011; Sinha et al., 2016).

Inflammation may also be maintained by HIV-1 itself. HIV-1 is not eliminated from the body after years of continuous suppressive therapy and viremia inevitably rebounds upon drug cessation (Davey et al., 1999). This is because HIV-1 establishes a provirus in long-lived $CD4^+$ memory T cells and perhaps other cell types that include tissue-resident myeloid cells (Jiang et al., 2015; Kandathil et al., 2016; Siliciano et al., 2003). Proviruses are obligate replication intermediates that integrate into chromosomal DNA to become permanent, heritable genetic elements in infected cells. Though the vast majority of proviruses that persist in the presence of antiviral therapy are defective for the production of infectious virus (Bruner et al., 2016), 2-18% express HIV-1 RNA (Wiegand et al., 2017). Here we assessed HIV-1 proviruses and their gene products for the ability to contribute to chronic inflammation.

RESULTS

To determine if HIV-1 proviruses activate innate immune signaling, human blood cells were transduced with single-cycle vectors, either a full-length, single-cycle HIV-1 clone with a frameshift in *env* and eGFP in place of *nef* (HIV-1-GFP) (He et al., 1997), or a minimal 3-part lentivector encoding GFP (Fig. 1A and Table 1) (Pertel et al., 2011). Monocyte derived dendritic cells (DCs) were challenged initially since HIV-1 transduction of these specialized antigen-presenting cells has been reported to activate innate immune signaling (Berg et al., 2012; Gao et al., 2013; Landau, 2014; Manel et al., 2010; Rasaiyaah et al., 2013). To increase the efficiency of provirus establishment, vectors were pseudotyped with the vesicular stomatitis virus glycoprotein (VSV G) and delivered concurrently with virus-like particles (VLPs) bearing SIV_{MAC}251 Vpx (Fig. 1B), as previously described (Goujon et al., 2006; Pertel et al., 2011). Transduction efficiency, as determined by flow cytometry for GFP-positive cells, was routinely 30-60% (Fig. 1B), depending on the blood donor.

DCs matured in response to HIV-1-GFP transduction, as indicated by increased mean fluorescence intensity of cell surface HLA-DR and co-stimulatory molecules CD80 and CD86 (Sousa, 2006) (Fig. 1B and C). Maturation was evident among both GFP positive and negative cells (Fig. 1B), the latter likely resulting from activation *in trans* by soluble mediators of inflammation (Manel et al., 2010; Rasaiyaah et al., 2013). Steady-state *CXCL10*, *IFNB1*, and *IL15* mRNAs reached maximum levels 48 hrs post-transduction, increasing 31,000-, 92-, and 140-fold relative to mock-treated cells, respectively (Fig. 1D and E). Correspondingly, IFNα2, CCL7, IL-6, CXCL10, and TNFα proteins accumulated in the supernatant (Fig. 1F). In contrast to the results with HIV-1-GFP, there were no signs of maturation after transduction with the 3-part minimal lentivector (Fig. 1B, D-F).

To determine if steps early in the HIV-1 replication cycle were necessary for maturation, reverse transcription was inhibited by nevirapine (NVP) or the HIV-1 RT mutant D185K/D186L, and integration was inhibited with raltegravir or the HIV-1 IN mutant D116A (Tables 1 and 2). Each of these four conditions abrogated maturation, as

indicated by cell surface CD86 (Fig. 1G) and steady-state *CXCL10* mRNA (Fig. 1H). *CXCL10* mRNA was detectable when integration was inhibited but levels were nearly 1,000 times lower than when HIV-1-GFP integration was not blocked.

HIV-1 virion RNA and newly synthesized viral cDNA have been reported to be detected by RIG-I or by cGAS, respectively (Berg et al., 2012; Gao et al., 2013). Both sensors activate signal transduction via TBK1 and IRF3. The TBK1 inhibitor BX795 (Table 2) blocked DC maturation in response to cGAMP but had no effect on maturation after HIV-1-GFP transduction (Fig. 1I). Similarly, prior knockdown of IRF3 using lentivectors (Table 1) (Pertel et al., 2011) suppressed activation in response to cGAMP but had no effect on HIV-1-induced maturation (Fig. 1I). Under the conditions used here, then, DC maturation required both reverse transcription and integration and was independent of TBK1 and IRF3.

Completion of the HIV-1 integration reaction requires cellular DNA repair enzymes (Craigie and Bushman, 2012). That DCs did not mature in response to transduction with minimal lentivectors (Fig. 1B, D-F) indicates that activation of the DNA repair process is not sufficient for maturation and that some product of HIV-1-GFP transcription must be necessary. Indeed, *gag* expression from an integrated vector has been reported to be necessary for DC maturation (Manel et al., 2010). To determine if any individual HIV-1 proteins were sufficient to mature DCs, a minimal lentivector was used to express codon optimized versions of each of the open reading frames possessed by HIV-1-GFP (Fig. 2A, Table 1). Among these vectors was a *gag*-expression vector that produced as much p24 protein as did HIV-1-GFP (Fig. 2A). None of these vectors matured DCs (Fig. 2A).

HIV-1-GFP protein coding sequences were then mutated to determine if any were necessary for DC maturation. Mutations that disrupted both *gag* and *pol*, either a double frameshift in *gag*, or a mutant in which the first 14 ATGs in *gag* were mutated, abolished synthesis of p24 but retained full maturation activity (Fig. 2B, Table 1). Deletion mutations encompassing *gag*/*pol*, *vif*/*vpr*, *vpu*/*env*, or *nef*/U3-LTR, each designed so as

to leave *cis*-acting RNA elements intact, all matured DCs (Fig. 2C and Table 1), indicating that these HIV-1-GFP RNA sequences, as well as the proteins that they encode, were not required for DC maturation.

Tat and Rev coding sequences were individually disrupted by combining start codon point mutations with nonsense codons that were silent with respect to overlapping reading frames (Table 1). Neither Δ*tat* nor Δ*rev* matured DCs upon transduction (Fig. 2D). However, DCs matured upon co-transduction of Δ*tat* with Δ*rev*, or when minimal lentivectors expressing codon-optimized Tat and Rev *in trans* were co-transduced (Fig. 2D). These results indicate that the maturation defect with the individual vectors was due to disruption of Tat and Rev function, and that, if expressed, the mutant RNAs matured DCs.

The minimal 3-part lentivector expressed GFP from a heterologous promoter and had a deletion mutation encompassing the essential, *cis*-acting TATA box and enhancer elements (Zufferey et al., 1998), as well as in the *trans*-acting *tat* and *rev*, that inactivated the promoter in the proviral 5' LTR (Fig. 1A). To test the importance of LTR-driven transcription for DC maturation by the HIV-1 provirus, the HIV-1 LTR was restored in the minimal vector (Fig. 2E and Table 1); in addition, GFP was inserted in place of *gag* as a marker for LTR expression, and the heterologous promoter was used to drive *tat*, *rev*, or both genes separated by P2A coding sequence (Fig. 2E). None of the LTR-driven, minimal vectors matured DCs (Fig. 2E).

To determine if *tat* was necessary for DC maturation, *tat* and TAR were mutated in HIV-1-GFP and the LTR promoter was modified to be tetracycline-inducible, as previously described (Das and Berkhout, 2016) (Tet-HIV-1 in Fig. 3A and Table 1). The doxycycline-dependent reverse transactivator (*rtTA*) was delivered by lentivector *in trans*. In the presence of doxycycline (Table 2), Tet-HIV-1 and rtTA in combination, but neither vector in isolation, matured DCs (Fig. 3A). This result demonstrated that, so long as the provirus is expressed, *tat* was not required for maturation. Additionally, the

magnitude of cell surface CD86 was dependent on the doxycycline concentration, indicating that maturation was dependent on the level of HIV-1 transcription (Fig. 3B).

To ascertain whether *rev* was necessary for DC maturation, the RTE from a murine intracisternal A-particle retroelement (IAP) and the CTE from SRV-1 were inserted in place of *nef* (HIV-RTE/CTE in Fig. 3C and Table 1) (Smulevitch et al., 2006). Each of these elements utilizes the NXF1 nuclear RNA export pathway, thereby bypassing the need for CRM1 and *rev (Fornerod et al., 1997)*. p24 levels with this construct were similar to those of HIV-1-GFP, indicating that nuclear export of unspliced RNA was comparable (Fig. 3C). Nonetheless, the HIV-RTE/CTE vector did not mature DCs (Fig. 3C), indicating that maturation was dependent upon *rev* and CRM1-mediated RNA export. Consistent with this conclusion, the CRM1 inhibitor leptomycin B (Table 2) abrogated DC maturation by HIV-1-GFP (Fig. 3D). In contrast, leptomycin B had no effect on DC maturation in response to infection with Sendai virus or yellow fever virus (Fig. 3E). ISG15 was used to monitor maturation in these experiments since, as previously reported for DCs, leptomycin B altered background levels of CD86 (Chemnitz et al., 2010).

To determine if innate immune detection of HIV-1 was unique to DCs, monocyte-derived macrophages and $CD4^+$ T cells were examined. In response to transduction with HIV-1-GFP, macrophages upregulated CD86, ISG15, and HLA-DR, and $CD4^+$ T cells upregulated MX1, IFIT1 and HLA-DR (Fig. 4A). DCs, macrophages, and $CD4^+$ T cells were then transduced side-by-side with mutant constructs to determine if the mechanism of innate immune activation was similar to that in DCs. As with DCs, HIV-1-GFP bearing the Δ*gag/pol* deletion activated macrophages and $CD4^+$ T cells (Fig. 4B). Also in agreement with the DC results, neither the minimal lentivector, nor HIV-1-GFP bearing mutations in *integrase*, *tat*, or *rev*, matured any of the three cell types (Fig. 4B). Finally, to test the effect of HIV-1 proviral RNA on non-activated T cells, $CD4^+$ T cells were co-transduced with Tet-HIV-1 and the rtTA3 vector and cultured for 9 days in the absence of stimulation. Upon doxycycline treatment, T cells expressed GFP and MX1 (Fig. 4C). As in DCs, dose-dependent activation was observed with doxycycline (Fig.

4C). Together these data indicate that innate immune activation of all three cell types by HIV-1 requires integration, transcription, and Rev-dependent, HIV-1 intron-containing RNA.

DISCUSSION

The HIV-1 LTR generates a single primary transcript that gives rise to over 100 alternatively spliced RNAs (Ocwieja et al., 2012). The full-length, unspliced, intron-bearing transcript acts as viral genomic RNA in the virion and as mRNA for essential *gag*- and *pol*-encoded proteins. Expression of the unspliced transcript requires specialized viral and cellular machinery, HIV-1 Rev and CRM1 (Fornerod et al., 1997), in order to escape from the spliceosome. Results here indicate that unspliced or partially spliced HIV-1 RNA is detected by human cells as a danger signal, as has been reported for inefficiently spliced mRNAs from transposable elements in distantly related eukaryotes (Dumesic et al., 2013). Indeed, transposable elements are mutagenic to the host genome and it stands to reason that characteristic molecular features such as transcripts bearing multiple, inefficient splice signals would be detected by, and activate, innate immune signaling pathways.

The replication competent HIV-1 reservoir in memory $CD4^+$ T cells has a 44 wk half-life and thus necessitates life-long antiviral therapy (Crooks et al., 2015). Long-lived, replication competent HIV-1 reservoirs in other cell types have not been clearly demonstrated but may also play a role (Kandathil et al., 2016). The common genetic determinants in HIV-1 for maturation of $CD4^+$ T cells, macrophages, and DCs suggests that HIV-1 is detected by a mechanism that is conserved across cell types and that this mechanism would be active in any cell type that possesses and is capable of transcribing a provirus. Data here show that proviruses need not be replication competent to contribute to inflammation. Ongoing efforts to develop new drugs that block HIV-1 transcription, tat-mediated transcriptional elongation, or Rev-mediated preservation of unspliced transcripts (Mousseau et al., 2015), would be predicted to limit inflammation, and to offer an important addition to current anti-HIV-1 drug cocktails.

MATERIALS AND METHODS

Cell culture. Cells were cultured at 37°C in 5% CO_2 humidified incubators. HEK293E (Pertel et al., 2011) were maintained in DMEM supplemented with 10% FBS, 20 mM L-glutamine (ThermoFisher), 25 mM HEPES pH 7.2 (SigmaAldrich), 1 mM sodium pyruvate (ThermoFisher), and 1x MEM non-essential amino acids (ThermoFisher). Cytokine conditioned media was produced from HEK293 cells stably transduced with pAIP-hGMCSF-co (Addgene #74168), pAIP-hIL4-co (Addgene #74169), or pAIP-hIL2 (Addgene #90513), as previously described (Pertel et al., 2011).

Leukopaks were obtained from anonymous, healthy, blood bank donors (New York Biologics) after review by the UMMS IRB, according to NIH guidelines: http://grants.nih.gov/grants/policy/hs/faqs_aps_definitions.htm. PBMCs were isolated from leukopaks by gradient centrifugation on Histopaque-1077 (Sigma-Aldrich). $CD14^+$ mononuclear cells were isolated via positive selection using anti-CD14 antibody microbeads (Miltenyi). Enrichment for $CD14^+$ cells was routinely >95%.

To generate DCs or macrophages, $CD14^+$ cells were plated at a density of 1 to 2 x 10^6 cells/ml in RPMI-1640 supplemented with 5% heat inactivated human AB^+ serum (Omega Scientific, Tarzana, CA), 20 mM L-glutamine, 25 mM HEPES pH 7.2, 1 mM sodium pyruvate, and 1x MEM non-essential amino acids (RPMI-HS complete) in the presence of cytokines that promote differentiation. DCs were generated by culturing monocytes for 6 days in the presence of 1:100 cytokine-conditioned media containing human GM-CSF and human IL-4. DC preparations were consistently >99% DC-$SIGN^{high}$, $CD11c^{high}$, and $CD14^{low}$ by flow cytometry. Macrophages were generated by culturing for 7 days with GM-CSF conditioned media in the absence of IL-4. $CD4^+$ T cells were isolated from PBMCs that had been depleted of $CD14^+$ cells, as above, using anti-CD4 microbeads (Miltenyi). $CD4^+$ T cells were then cultured in RPMI-1640 supplemented with 10% heat inactivated FBS, 20 mM L-glutamine, 25 mM HEPES pH 7.2, 1 mM sodium pyruvate, 1x MEM non-essential amino acids (RPMI-FBS complete), and 1:2000 IL-2 conditioned media.

HIV-1 vector production. HEK293E cells were seeded at 75% confluency in 6-well plates and transfected with 6.25 uL Transit LT1 lipid reagent (Mirus) in 250 µL Opti-MEM (Gibco) with 2.25 µg total plasmid DNA. 2-part HIV-1 vectors based on HIV-1-GFP (He et al., 1997) and described in detail in Table 1 were transfected at a 7:1 ratio in terms of µgs of HIV-1 plasmid DNA to pMD2.G VSV G expression plasmid DNA (Pertel et al., 2011). 3-part lentivectors were produced by transfection of the lentivector genome, psPAX2 GagPol vector, and pMD2.G, at a DNA ratio of 4:3:1. VPX-bearing SIV-VLPs were produced by transfection at a 7:1 plasmid ratio of SIV3+ to pMD2.G (Pertel et al., 2011). 12 hrs after transfection, media was changed to the specific media for the cells that were to be transduced. Viral supernatant was harvested 2 days later, filtered through a 0.45 µm filter, and stored at 4°C.

Virions in the transfection supernatant were quantified by a PCR-based assay for reverse transcriptase activity (Pertel et al., 2011). 5 µl transfection supernatant were lysed in 5 µL 0.25% Triton X-100, 50 mM KCl, 100 mM Tris-HCl pH 7.4, and 0.4 U/µl RNase inhibitor (RiboLock, ThermoFisher). Viral lysate was then diluted 1:100 in a buffer of 5 mM $(NH_4)_2SO_4$, 20 mM KCl, and 20 mM Tris–HCl pH 8.3. 10 µL was then added to a single-step, RT PCR assay with 35 nM MS2 RNA (IDT) as template, 500 nM of each primer (5'-TCCTGCTCAACTTCCTGTCGAG-3' and 5'-CACAGGTCAAACCTCCTAGGAATG-3'), and hot-start Taq (Promega) in a buffer of 20 mM Tris-Cl pH 8.3, 5 mM $(NH_4)_2SO_4$, 20 mM KCl, 5 mM $MgCl_2$, 0.1 mg/ml BSA, 1/20,000 SYBR Green I (Invitrogen), and 200 µM dNTPs. The RT-PCR reaction was carried out in a Biorad CFX96 cycler with the following parameters: 42°C 20 min, 95°C 2 min, and 40 cycles [95°C for 5 s, 60°C 5 s, 72°C for 15 s and acquisition at 80°C for 5 s]. 2 part vectors typically yielded 10^7 RT units/µL, and 3 part vector transfections yielded 10^6 RT units/µL.

Transductions. 10^6 DCs/mL, or 5 x 10^5 macrophages/ml, were plated into RPMI-HS complete with Vpx^+ SIV-VLP transfection supernatant added at a dilution of 1:6. After 2 hrs, 10^8 RT units of viral vector was added. In some cases, drugs were added to the

culture media as specified in Table 2. In most cases, transduced DC were harvested for analysis 3 days following challenge. For gene knockdown or for expression of factors *in trans*, 2 x 10^6 $CD14^+$ monocytes/mL were transduced directly following magnetic bead isolation with 1:6 volume of SIV-VLPs and 1:6 volume of vector. When drug selection was required, 4 µg/mL puromycin was added 3 days after monocyte transduction and cells were selected for 3 days. SIV-VLPs were re-administered in all cases with HIV-1 or lentivector challenge. For DCs in Tet-HIV-1 experiments, fresh monocytes were SIV-VLP treated and co-transduced with rtTA3 and Tet-HIV-1. DCs were harvested 6 days later and treated with indicated doxycycline concentrations.

$CD4^+$ T cells were stimulated in RPMI-FBS complete with 1:2000 hIL-2 conditioned media and 5 µg/mL PHA-P. After 3 days, T cells were replated at 10^6 cells/mL in RPMI-FBS complete with hIL-2. Cells were transduced with 10^8 RT units of viral vector per 10^6 cells and assayed 3 days later. T cells were co-transduced with rtTA3 and Tet-HIV-1 every day for 3 days after PHA stimulation. Cells were then replated in RPMI-FBS complete with hIL-2. Transduced T cells were cultured for 9 days with fresh media added at day 5. After 9 days, doxycycline was added at the indicated concentrations and assayed 3 days later.

Cytokine analysis. Supernatants from DCs were collected 3 days following transduction with HIV-1-GFP or minimal lentivector. Supernatant was spun at 500 x g for 5 mins and filtered through a 0.45 µm filter. Multiplex soluble protein analysis was carried out by Eve Technologies (Calgary, AB, Canada).

qRT-PCR. Total RNA was isolated from 5 x 10^5 DCs using RNeasy Plus Mini (Qiagen) with Turbo DNase (ThermoFisher) treatment between washes. First-strand synthesis used Superscript III Vilo Master mix (Invitrogen) with random hexamers. qPCR was performed in 20 µL using 1× TaqMan Gene Expression Master Mix (Applied Biosystems), 1 µL cDNA, and 1 µL TaqMan Gene Expression Assays (ThermoFisher) specified in Table 3. Amplification was on a CFX96 Real Time Thermal Cycler (Bio-Rad)

using the following program: 95°C for 10 min [45 cycles of 95°C for 15 s and 60°C for 60 s]. Housekeeping gene OAZ1 was used as control (Pertel et al., 2011).

Flow cytometry. 10^5 cells were surface stained in FACS buffer (PBS, 2% FBS, 0.1% Sodium Azide), using the antibodies in Table 4. Cells were then fixed in a 1:4 dilution of BD Fixation Buffer and assayed on a BD C6 Accuri. BD Biosciences Fixation and Permeabilization buffers were utilized for intracellular staining. Data was analyzed in FlowJo.

ACKNOWLEDGEMENTS

We thank the 256 anonymous blood donors who contributed leukocytes to this project, and Ben Berkhout, Abraham Brass, Barbara Felber, Massimo Pizzato, and Didier Trono for advice and reagents. This work was supported by NIH Grants 5R01AI111809, 5DP1DA034990, and 1R01AI117839, to J.L. The plasmids described in Table 1, along with their complete nucleotide sequences, are available at www.addgene.com.

REFERENCES

Berg, R.K., Melchjorsen, J., Rintahaka, J., Diget, E., Søby, S., Horan, K.A., Gorelick, R.J., Matikainen, S., Larsen, C.S., Ostergaard, L., et al. (2012). Genomic HIV RNA induces innate immune responses through RIG-I-dependent sensing of secondary-structured RNA. PLoS One *7*, e29291.

Brenchley, J.M., Price, D.A., Schacker, T.W., Asher, T.E., Silvestri, G., Rao, S., Kazzaz, Z., Bornstein, E., Lambotte, O., Altmann, D., et al. (2006). Microbial translocation is a cause of systemic immune activation in chronic HIV infection. Nat. Med. *12*, 1365–1371.

Bruner, K.M., Murray, A.J., Pollack, R.A., Soliman, M.G., Laskey, S.B., Capoferri, A.A., Lai, J., Strain, M.C., Lada, S.M., Hoh, R., et al. (2016). Defective proviruses rapidly accumulate during acute HIV-1 infection. Nat. Med. *22*, 1043–1049.

Chemnitz, J., Turza, N., Hauber, I., Steinkasserer, A., and Hauber, J. (2010). The karyopherin CRM1 is required for dendritic cell maturation. Immunobiology *215*, 370–379.

Craigie, R., and Bushman, F.D. (2012). HIV DNA integration. Cold Spring Harb. Perspect. Med. *2*, a006890.

Crooks, A.M., Bateson, R., Cope, A.B., Dahl, N.P., Griggs, M.K., Kuruc, J.D., Gay, C.L., Eron, J.J., Margolis, D.M., Bosch, R.J., et al. (2015). Precise quantitation of the latent HIV-1 reservoir: implications for eradication strategies. J. Infect. Dis. *212*, 1361–1365.

Das, A.T., and Berkhout, B. (2016). Conditionally replicating HIV and SIV variants. Virus Res. *216*, 66–75.

Davey, R.T., Jr, Bhat, N., Yoder, C., Chun, T.W., Metcalf, J.A., Dewar, R., Natarajan, V., Lempicki, R.A., Adelsberger, J.W., Miller, K.D., et al. (1999). HIV-1 and T cell dynamics after interruption of highly active antiretroviral therapy (HAART) in patients with a history of sustained viral suppression. Proc. Natl. Acad. Sci. U. S. A. *96*, 15109–15114.

Dumesic, P.A., Natarajan, P., Chen, C., Drinnenberg, I.A., Schiller, B.J., Thompson, J., Moresco, J.J., Yates, J.R., 3rd, Bartel, D.P., and Madhani, H.D. (2013). Stalled spliceosomes are a signal for RNAi-mediated genome defense. Cell *152*, 957–968.

Fornerod, M., Ohno, M., Yoshida, M., and Mattaj, I.W. (1997). CRM1 is an export receptor for leucine-rich nuclear export signals. Cell *90*, 1051–1060.

Freiberg, M.S., Chang, C.-C.H., Kuller, L.H., Skanderson, M., Lowy, E., Kraemer, K.L., Butt, A.A., Bidwell Goetz, M., Leaf, D., Oursler, K.A., et al. (2013). HIV infection and the risk of acute myocardial infarction. JAMA Intern. Med. *173*, 614–622.

Gao, D., Wu, J., Wu, Y.-T., Du, F., Aroh, C., Yan, N., Sun, L., and Chen, Z.J. (2013). Cyclic GMP-AMP synthase is an innate immune sensor of HIV and other retroviruses. Science *341*, 903–906.

Goujon, C., Jarrosson-Wuillème, L., Bernaud, J., Rigal, D., Darlix, J.-L., and Cimarelli, A. (2006). With a little help from a friend: increasing HIV transduction of monocyte-derived dendritic cells with virion-like particles of SIV(MAC). Gene Ther. *13*, 991–994.

Günthard, H.F., Saag, M.S., Benson, C.A., del Rio, C., Eron, J.J., Gallant, J.E., Hoy, J.F., Mugavero, M.J., Sax, P.E., Thompson, M.A., et al. (2016). Antiretroviral Drugs for Treatment and Prevention of HIV Infection in Adults: 2016 Recommendations of the International Antiviral Society-USA Panel. JAMA *316*, 191–210.

He, J., Chen, Y., Farzan, M., Choe, H., Ohagen, A., Gartner, S., Busciglio, J., Yang, X., Hofmann, W., Newman, W., et al. (1997). CCR3 and CCR5 are co-receptors for HIV-1 infection of microglia. Nature *385*, 645–649.

Hunt, P.W., Martin, J.N., Sinclair, E., Epling, L., Teague, J., Jacobson, M.A., Tracy, R.P., Corey, L., and Deeks, S.G. (2011). Valganciclovir reduces T cell activation in HIV-infected individuals with incomplete CD4+ T cell recovery on antiretroviral therapy. J. Infect. Dis. *203*, 1474–1483.

Jiang, A.-P., Jiang, J.-F., Wei, J.-F., Guo, M.-G., Qin, Y., Guo, Q.-Q., Ma, L., Liu, B.-C., Wang, X., Veazey, R.S., et al. (2015). Human Mucosal Mast Cells Capture HIV-1 and

Mediate Viral trans-Infection of CD4+ T Cells. J. Virol. *90*, 2928–2937.

Kandathil, A.J., Sugawara, S., and Balagopal, A. (2016). Are T cells the only HIV-1 reservoir? Retrovirology *13*, 86.

Landau, N.R. (2014). The innate immune response to HIV-1: to sense or not to sense. DNA Cell Biol. *33*, 271–274.

Manel, N., Hogstad, B., Wang, Y., Levy, D.E., Unutmaz, D., and Littman, D.R. (2010). A cryptic sensor for HIV-1 activates antiviral innate immunity in dendritic cells. Nature *467*, 214–217.

Mousseau, G., Kessing, C.F., Fromentin, R., Trautmann, L., Chomont, N., and Valente, S.T. (2015). The Tat Inhibitor Didehydro-Cortistatin A Prevents HIV-1 Reactivation from Latency. MBio *6*, e00465.

Ocwieja, K.E., Sherrill-Mix, S., Mukherjee, R., Custers-Allen, R., David, P., Brown, M., Wang, S., Link, D.R., Olson, J., Travers, K., et al. (2012). Dynamic regulation of HIV-1 mRNA populations analyzed by single-molecule enrichment and long-read sequencing. Nucleic Acids Res. *40*, 10345–10355.

Pertel, T., Hausmann, S., Morger, D., Züger, S., Guerra, J., Lascano, J., Reinhard, C., Santoni, F.A., Uchil, P.D., Chatel, L., et al. (2011). TRIM5 is an innate immune sensor for the retrovirus capsid lattice. Nature *472*, 361–365.

Rasaiyaah, J., Tan, C.P., Fletcher, A.J., Price, A.J., Blondeau, C., Hilditch, L., Jacques, D.A., Selwood, D.L., James, L.C., Noursadeghi, M., et al. (2013). HIV-1 evades innate immune recognition through specific cofactor recruitment. Nature *503*, 402–405.

Siliciano, J.D., Kajdas, J., Finzi, D., Quinn, T.C., Chadwick, K., Margolick, J.B., Kovacs, C., Gange, S.J., and Siliciano, R.F. (2003). Long-term follow-up studies confirm the stability of the latent reservoir for HIV-1 in resting CD4+ T cells. Nat. Med. *9*, 727–728.

Sinha, A., Ma, Y., Scherzer, R., Hur, S., Li, D., Ganz, P., Deeks, S.G., and Hsue, P.Y. (2016). Role of T-Cell Dysfunction, Inflammation, and Coagulation in Microvascular

Disease in HIV. J. Am. Heart Assoc. *5*, e004243.

Smulevitch, S., Bear, J., Alicea, C., Rosati, M., Jalah, R., Zolotukhin, A.S., von Gegerfelt, A., Michalowski, D., Moroni, C., Pavlakis, G.N., et al. (2006). RTE and CTE mRNA export elements synergistically increase expression of unstable, Rev-dependent HIV and SIV mRNAs. Retrovirology *3*, 1–9.

Sousa, C.R. e. (2006). Dendritic cells in a mature age. Nat. Rev. Immunol. *6*, 476–483.

Wiegand, A., Spindler, J., Hong, F.F., Shao, W., Cyktor, J.C., Cillo, A.R., Halvas, E.K., Coffin, J.M., Mellors, J.W., and Kearney, M.F. (2017). Single-cell analysis of HIV-1 transcriptional activity reveals expression of proviruses in expanded clones during ART. Proc. Natl. Acad. Sci. U. S. A. *114*, E3659–E3668.

Zufferey, R., Dull, T., Mandel, R.J., Bukovsky, A., Quiroz, D., Naldini, L., and Trono, D. (1998). Self-inactivating lentivirus vector for safe and efficient in vivo gene delivery. J. Virol. *72*, 9873–9880.

FIGURE LEGENDS

Fig. 1. HIV-1 transduction matures DCs. (A) Schematics of HIV-1-GFP, with frameshift in *env* (red line) and *gfp* in place of *nef* (He et al., 1997), and the minimal lentivector, with self-inactivating ΔU3 LTR (Zufferey et al., 1998) and *gfp* driven by the SFFV promoter (Pertel et al., 2011). (**B**) Flow cytometry of DCs for GFP and CD86, after treatment as indicated. **(C)** Flow cytometry histograms for the indicated markers 72 hrs after DC transduction with HIV-1 (red) or mock (black). **(D)** qRT-PCR quantitation of *CXCL10* mRNA in DCs transduced with either HIV-1-GFP or minimal lentivector in the presence of Vpx, and assessed at the indicated times post-transduction. **(E)** qRT-PCR quantitation of *CXCL10* (black), *IFNB1* (gray), or *IL15* (white) mRNAs from DCs transduced with HIV-1-GFP. **(F)** Cytokines in DC supernatant as assessed by luminex, 72 hrs after transduction with HIV-1-GFP (black) or minimal lentivector (gray). **(G)** Assessment of GFP and CD86 by flow cytometry following transduction with [Top] HIV-1-GFP in the presence of 5 µM nevirapine (RTi), 10 µM raltegravir (INi), or no drug, [Bottom] HIV-1-GFP bearing mutant RT-D185K/D186L (RTmut) or mutant IN-D116A (INmut). (**H**) qRT-PCR quantitation of *CXCL10* mRNA from the same DCs as in (**G**). **(I)** DCs treated with 1 µM of the TBK1 inhibitor BX795, or expressing shRNAs targeting either IRF3 or luciferase control (Pertel et al., 2011), were challenged with 25 µg/mL cGAMP or HIV-1-GFP and assayed by flow cytometry for CD86.

Fig. 2. Native HIV-1 RNA regulation is necessary for DC maturation, but LTR-driven transcription is insufficient and coding sequences are not necessary. Flow cytometry of DCs after transduction with **(A)** minimal lentivectors expressing codon optimized HIV-1 genes; **(B)** HIV-1-GFP in which translation was disrupted by two frameshifts in *gag* or by mutation of the first 14 AUGs in *gag*; **(C)** HIV-1-GFP bearing deletion mutations encompassing *gag*/*pol*, *vif*/*vpr*, *vpu*/*env*, or *nef*/U3-LTR; **(D)** HIV-1-GFP bearing mutations in *tat* or *rev*, co-transduced with both mutants, or co-transduced with minimal vector expressing *tat* and *rev in trans*; or **(E)** minimal lentivector with GFP in place of *gag*, SFFV promoter driving expression of *tat*, *rev*, or both, and repaired U3 in the 3' LTR; the latter restores 5'-LTR-directed transcription to the provirus as a result of the reverse transcription strand-transfer reactions.

Fig. 3. Rev-mediated RNA export is necessary for DC maturation but Tat is dispensable. (**A**) Optimized 2xTet operator (Das and Berkhout, 2016) was cloned into the 3'LTR of HIV-1-GFPΔ*tat* to generate Tet-HIV-1; the strand-transfer reactions that occur during reverse transcription generate a Tet-regulated 5'-LTR in the provirus. DCs transduced with Tet-HIV-1, rtTA3, or both, were treated for 3 d with 500 ng/mL doxycycline and assayed by flow cytometry for p24, GFP, and CD86. (**B**) DCs co-transduced with Tet-HIV-1 and rtTA3 were treated with increasing concentrations of doxycycline. (**C**) To generate HIV-1-RTE/CTE, the RTEm26CTE element (Smulevitch et al., 2006) was cloned in place of *nef* in HIV-1-GFPΔ*rev*/ΔRRE. DCs were transduced with the indicated vectors and assessed for p24 and ISG15 by flow cytometry. (**D**) DCs were treated with 25 nM leptomycin B, transduced with HIV-1-GFP, and assessed for GFP and ISG15 by flow cytometry. (**E**) DCs were treated with 25 nM leptomycin B, transduced with HIV-1-GFP or infected with Sendai virus (SeV) or yellow fever virus (YFV), and assessed for ISG15 by flow cytometry.

Fig. 4. Innate immune activation in macrophages and $CD4^+$ T cells by HIV-1 proviral transcription. (**A**) Macrophages and $CD4^+$ T cells were transduced with HIV-1-GFP and assayed 3 days later for the indicated activation markers. (**B**) DCs, macrophages, and $CD4^+$ T cells were challenged with HIV-1-GFP or the indicated mutants. The upper panel shows flow cytometry of the DCs for GFP and CD86. The histograms show CD86 for DCs and macrophages or MX1 for $CD4^+$ T cells. (**C**) $CD4^+$ T cells were stimulated for 3 days with PHA and IL2, and transduced with Tet-HIV-1 and rtTA3. Cells were then cultured without stimulation for 9 days. Doxycycline was then added at the indicated concentrations. Cells were assayed for GFP and MX1 3 days later.

Table 1. Plasmids used in this study.

Plasmid Name	Purpose	Notes	Addgene code #
pBS NL4-3 *env*^{FS} eGFP	Single-cycle, full-length HIV-1	"HIV-1-GFP" in the manuscript. HIV-1 NL4-3 in pBluescript, flanking host sequences deleted, frameshift in *env*, eGFP in place of *nef*	pending
pMD2.G	VSV G	Pseudotype HIV-1 vectors with VSV G	12259
psPAX2	HIV-1 *gag-pol*	"3-part" lentivector or for complementation of assembly-incompetent HIV-1 vectors	12260
SIV3+	SIV_{MAC251} *gag-pol/vpx*	Production of SIV VLPs containing Vpx protein	pending
pALPS	Minimal lentivector	Includes *cis*-acting elements required for reverse transcription and integration, psi RNA packaging element, RRE, cPPT, PPT, mutation in the 3'LTR U3 that eliminates LTR-based transcription, and SFFV promoter to express genes of interest.	90996
pALPS eGFP	eGFP lentivector	Encodes eGFP	pending
pALPS *gag*	*gag* lentivector	Encodes codon optimized NL4-3 *gag*	pending
pALPS *env*	*env* lentivector	Encodes codon optimized JR-CSF *env*	pending
pALPS *tat*	*tat* lentivector	Encodes codon optimized NL4-3 *tat*	pending
pALPS *rev*	*rev* lentivector	Encodes codon optimized NL4-3 *rev*	pending
pALPS *vif*	*vif* lentivector	Encodes codon optimized NL4-3 *vif*	pending
pALPS *vpr*	*vpr lentivector*	Encodes codon optimized NL4-3 *vpr*	pending
pALPS *vpu*	*vpu lentivector*	Encodes codon optimized NL4-3 *vpu*	pending
pALPS *tat*-P2A-*rev*	*tat* and *rev lentivector*	Lentivector expressing codon optimized NL4-3 *tat* and *rev* linked by P2A peptide coding sequence (GSGATNFSLLKQAGDVEENPGP)	pending
pBS NL4-3 *env*^{FS} eGFP RT-D185K/D186L	RT mutant	pBS NL4-3 *env*^{FS} eGFP with mutation that disrupts Reverse Transcriptase catalytic activity	pending
pBS NL4-3 *env*^{FS} eGFP IN-D116A	IN mutant	pBS NL4-3 *env*^{FS} eGFP with mutation that disrupts IN catalytic activity	pending
pBS NL4-3 *env*^{FS} eGFP PR-D25A	PR mutant	pBS NL4-3 *env*^{FS} eGFP with mutation that disrupts Protease catalytic activity	pending
pALPS puro miR30-L1221	Luciferase knockdown	negative control for knockdowns target site: CTTGTCGATGAGAGCGTTTGT	pending
pALPS puro miR30-IRF3	IRF3 knockdown	target site ATCAGATCTACAATGAAGGGC	pending
pALPS_3'LTR GFP@gag start SFFV-	U3+ lentivector GFP at *gag* start SFFV promoter	Repaired U3 allows LTR-based transcription by the provirus with GFP as a marker for expression. WPRE was deleted.	pending
pALPS_3'LTR GFP@*gag* start SFFV *tat*	U3+ lentivector GFP at *gag* start SFFV-*tat*	LTR drives GFP and internal SFFV promoter drives codon optimized *tat*	pending
pALPS_3'LTR GFP@*gag* start SFFV *rev*	U3+ lentivector GFP at *gag* start SFFV-*rev*	LTR drives GFP and internal SFFV promoter drives codon optimized *rev*	pending

pALPS_3'LTR GFP@*gag* start SFFV *tat*-P2A-*rev*	U3+ lentivector with SFFV-*tatP2Arev*	LTR drives GFP and internal SFFV promoter drives codon optimized *tat* and *rev*.	pending
pNL4-3 *env*^{FS} eGFP *gag*^{2xFS}	No Gag synthesis	1st frameshift is CG nucleotide insertion in MA at nt 832. 2nd is a CTAG addition in CA at nt 1508.	pending
pNL4-3 *env*^{FS} eGFP NoStarts	No Gag synthesis	All ATGs from the start of *gag* to NC mutated to ATC except the first which was mutated to ACG	pending
pBS NL4-3 *env*^{FS} eGFP Δ*gag/pol*	*gag-pol* deletion	Deletion from the start of *gag* until 229 bases before the cPPT	pending
pNL4-3 *env*^{FS} eGFP Δ*vif/vpr*	*vif*/*vpr* deletion	Deletion from NL4-3 nt 5582-6199 encompassing Vif and Vpr coding sequence	pending
pNL4-3 *env*^{FS} eGFP Δ*vpu/env*	*vpu*/*env* deletion	Deletion from NL4-3 nt 6054-7489 encompassing all of *vpu* and *env* until before the RRE	pending
pBS NL4-3 *env*^{FS} eGFP Δ*nef*/U3	*nef*/U3 deletion	Deletion from NL4-3 nt 8911-9022 and 9088-9377. This deletes *nef* and U3 LTR sequences	pending
pBS NL4-3 *env*^{FS} eGFP 5'CMV Δ*tat*	HIV-1 with inactivating mutations in *tat*	*tat* ATG->ACG (silent in *vpr* reading frame), nt 78 mutated T->G to change Tyr to stop codon, nt 116 mutated T->C to disrupt Met, 5'LTR replaced with CMV-R-U5 from pALPS for *tat*-independent transcription in HEK293E cells.	pending
pBS NL4-3 *env*^{FS} eGFP Δ*rev*	HIV-1 with inactivating mutations in *rev*	All mutations in *rev* are silent with respect to the *tat* reading frame. Start ATG->ACG and nts 68-71 were mutated AGC->TCA to change tyrosine to a stop.	pending
pBS NL4-3 *env*^{FS} eGFP 5'CMV Δ*tat* ΔTARx2_d2TetOp	Tet-inducible, *tat*-independent HIV-1	2xTet Operator inserted between NFkB and Sp1 sites in U3 of HIV-1 Δ*tat* with 5' CMV-R-U5. 5' and 3' TAR elements were mutated to: 5'-GGTCTCTCTGGTTAGACCAGAAAGGAGCATTGGAGCTCTCTGGCTAACTAGGGAACCC-3'	pending
pALPS rtTA3_V14	rtTA3 lentivector	Codon optimized rtTA3 used *in trans* with Tet inducible HIV-1	pending
pSC101 NL4-3 *env*^{FS} Δ*rev* ΔRRE RTEm26CTE	Rev (CRM1) independent HIV-1	HIV-1 ΔRev was cloned into pSC101 and modified to include an RTEm26CTE element in order to utilize the NXF1 RNA export pathway. The RRE was also mutated.	pending

Table 2. Drugs and viruses.

Drug	Function	Source	Working concentration
Nevirapine	Reverse transcriptase inhibitor	NIH AIDS reagent program https://www.aidsreagent.org	5 µM
Raltegravir	Integrase inhibitor	NIH AIDS reagent program	10 µM
BX795	TBK1 inhibitor	InvivoGen (cat #tlrl-bx7)	1 µM
Leptomycin	CRM1 inhibitor	InvivoGen (cat #tlrl-lep)	25 nM
Doxycycline	rtTA3 activator	Sigma-Aldrich (D9891)	10-1000 ng/mL
cGAMP	STING activator	InvivoGen (cat #tlrl-nacga23)	25 µg/mL
PHA-P	T cell mitogen	Sigma-Aldrich (L1668)	5 µg/mL
Sendai Virus (SeV) Cantell strain	Challenge virus	Charles River Labs (VR-907)	1:100 dilution
Yellow Fever Virus (YFV) vaccine 17D	Challenge virus	Abraham Brass	1:100 dilution

Table 3. qRT-PCR probes.

RNA Target	Taqman probe ID#
CXCL10	Hs00171042_m1
IFNB1	Hs01077958_s1
IL15	Hs01003716_m1
OAZ1	Hs00427923_m1
ACTB	Hs01060665_g1

Table 4. Antibodies used in this study.

Target antigen	Clone	Fluorophore	Source
CD80	2D10	PE, APC	Biolegend
CD86	IT2.2	PE, APC	Biolegend
CD40	HB14	APC	Biolegend
HLA-DR	L249	PerCP, APC	Biolegend
CD83	HB15e	FITC, APC	Biolegend
CCR7	G043H7	PE	Biolegend
CD141	M80	PE	Biolegend
ISG15	#851701	PE, APC	R&D Systems
MX1	EPR19967	N/A	Abcam
IFIT	OTI3G8	N/A	Abcam
p24	KC57	FITC, PE	BeckmanCoulter
CD1a	HI149	FITC, PerCP	Biolegend
CD1c	L161	PE	Biolegend
CD14	HCD14	FITC, Pe-Cy7	Biolegend
CD11b	ICRF44	PE	Biolegend
CD11c	3.9	PE, PE-Cy7, APC	Biolegend
CD209 (DC-SIGN)	9E9A8	APC	Biolegend
CXCL10	JO34D6	PE	Biolegend
HLA-ABC	W6/32	FITC	Biolegend
CD3	OKT3	FITC, APC, BV650	Biolegend
CD4	OKT4	FITC, APC, Alexa700	Biolegend
Mouse-IgG	Poly4053	PE, APC	Biolegend
Rabbit-IgG	Poly4064	PE, AlexaFluor647	Biolegend

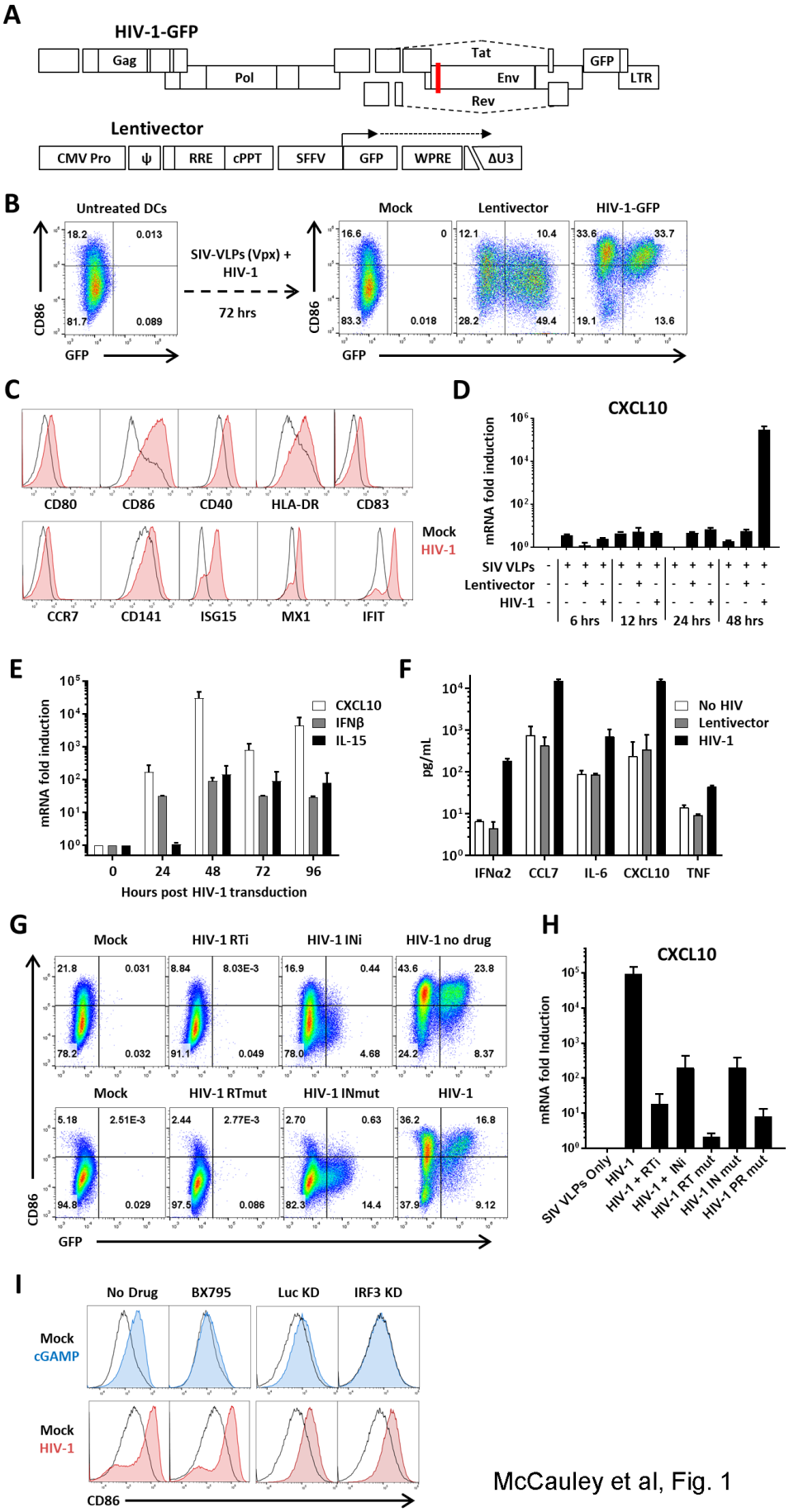

McCauley et al, Fig. 1

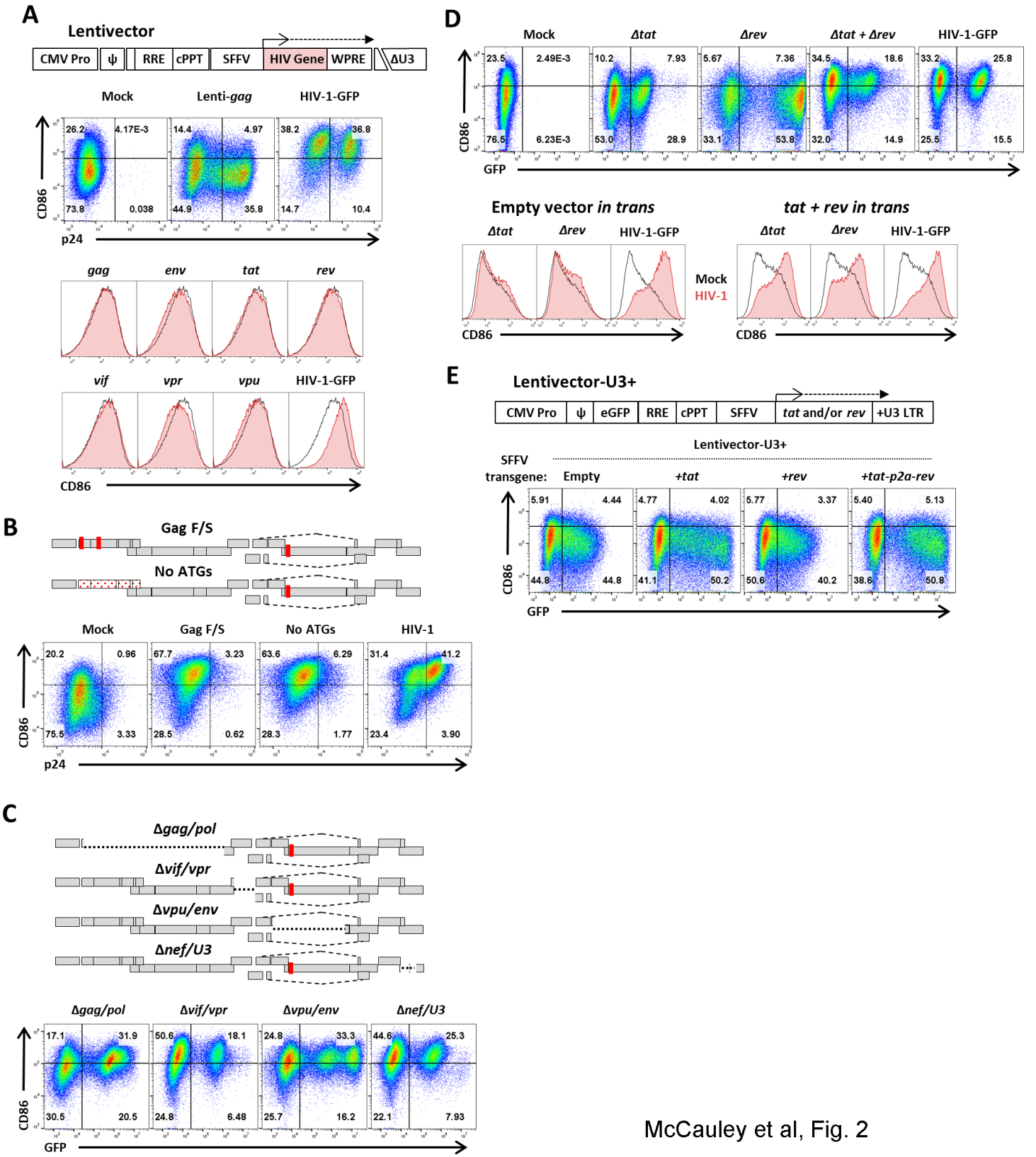

McCauley et al, Fig. 2

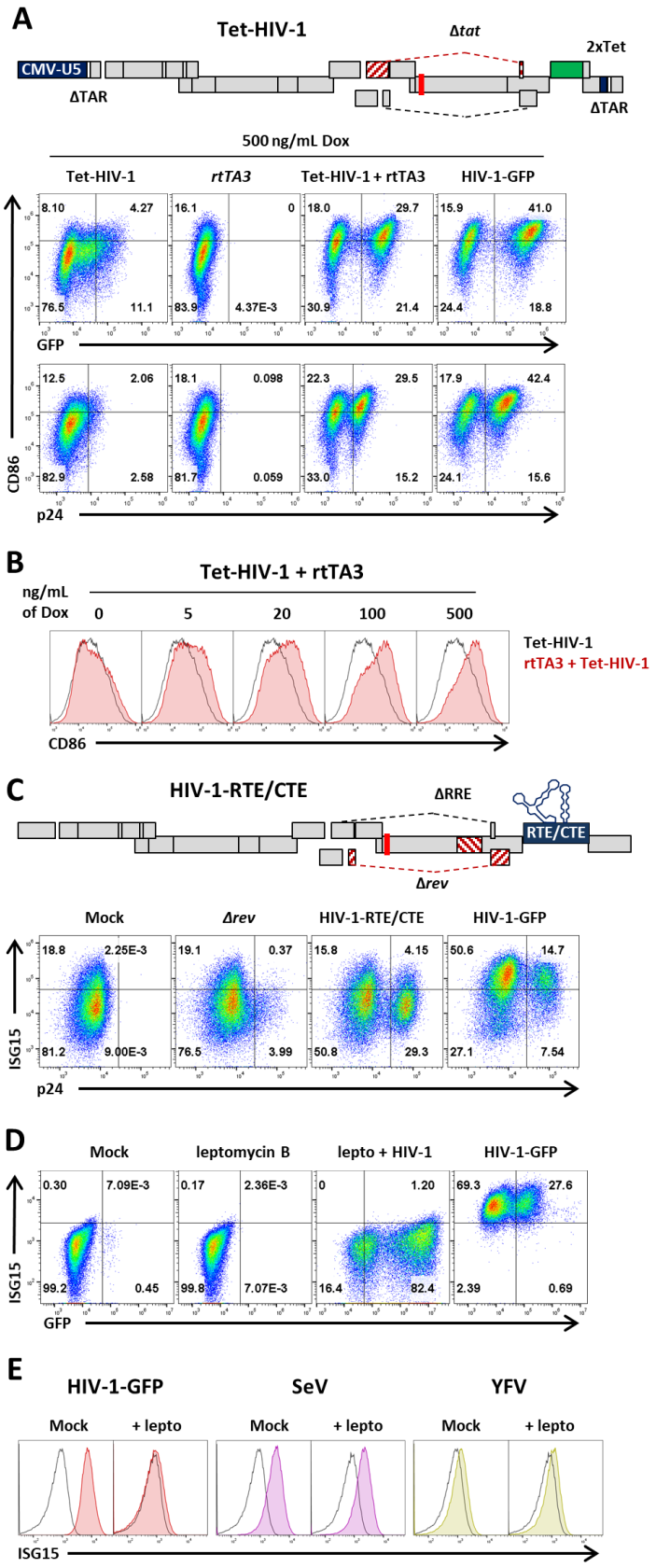

McCauley et al, Fig. 3

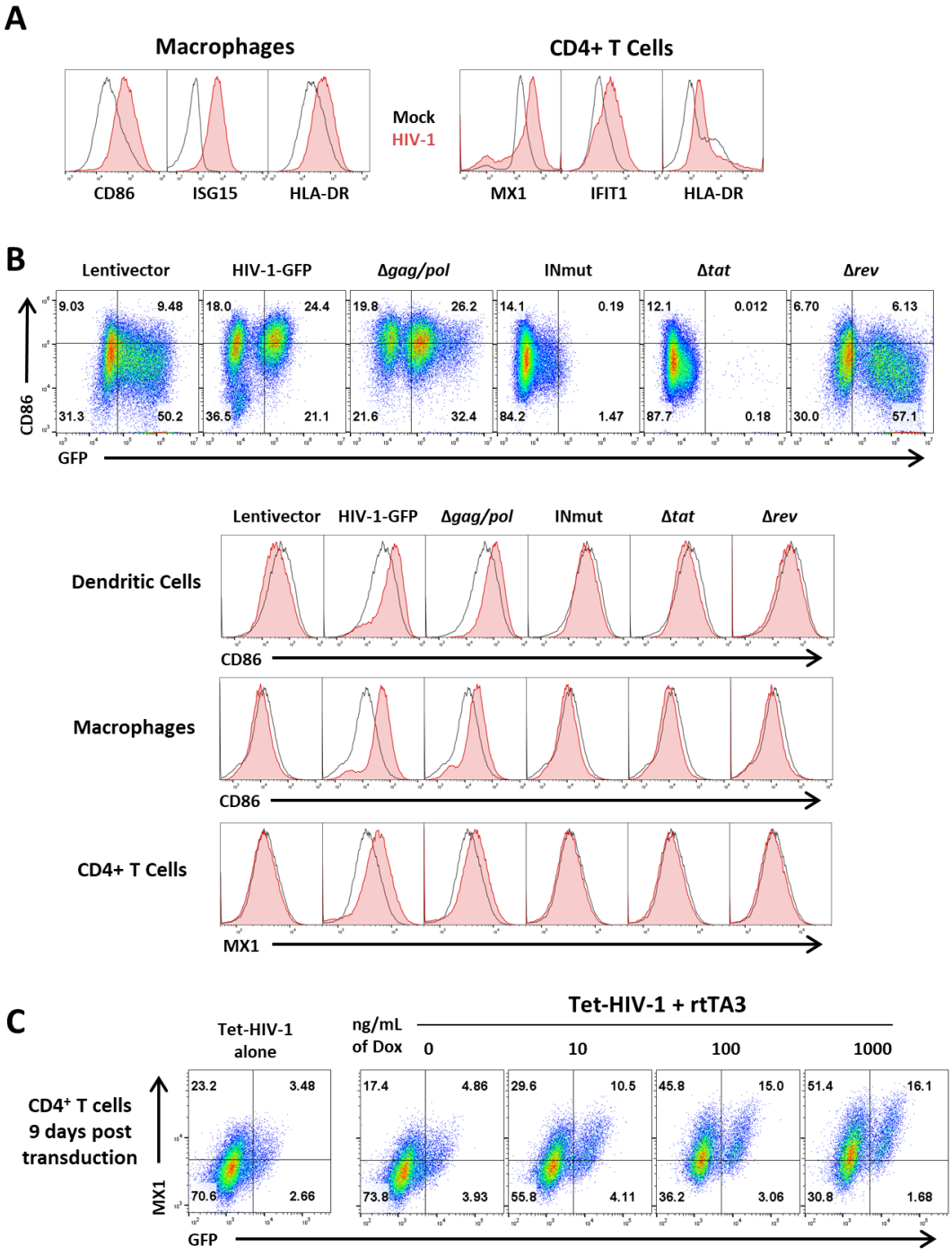

McCauley et al, Fig. 4